Available online at www.sciencedirect.com
SCIENCE DIRECT
Catalysis Today 109 (2005) 33–41
CATALYSIS TODAY
www.elsevier.com/locate/cattod

Supported (NiMo,CoMo)-carbide, -nitride phases: Effect of atomic ratios and phosphorus concentration on the HDS of thiophene and dibenzothiophene

L.A. Santillán-Vallejo [a], J.A. Melo-Banda [a,*], A.I. Reyes de la Torre [a], G. Sandoval-Robles [a], J.M. Domínguez [b], A. Montesinos-Castellanos [c], J.A. de los Reyes-Heredia [c]

[a] *Instituto Tecnológico de Ciudad Madero, División de Estudios de Posgrado e Investigación, Depto. de Ing. Química, J. Rosas y J. Urueta, C.P. 89440, Cd. Madero, Tamps., México, Mexico*
[b] *Instituto Mexicano del Petróleo, Programa de Ingeniería Molecular, Eje Central L. Cárdenas 152, 07730 México D.F., Mexico*
[c] *Universidad Autónoma Metropolitana-Iztapalapa, Departamento de Ingeniería de Procesos e Hidráulica, Av. Rafael Atlixco 186, Col Vicentina, Iztapalapa, 09340 México D.F., Mexico*

Abstract

A study on the catalytic properties of the transition metals (Ni,Co,Mo)-carbides, -nitrides for thiophene and dibenzothiophene hydrotreating was conducted. The (Ni,Co)-Mo carbides and the corresponding (Ni,Co)-Mo nitride phases showed a catalytic activity higher than conventional bimetallic (Ni,Co)-Mo sulfides. In addition, a study was done on the effect of the atomic ratios, i.e., $0.1 \leq M^+/(M^+ + Mo) \leq 0.9$ where M^+ stands for Ni or Co, and the concentration of promoters such as phosphorous, which was a structural stabilizing agent. The catalytic performance of the bimetallic NiMo and CoMo carbides and nitrides was studied using thiophene and dibenzothiophene hydrodesulfurization (HDS) as model reactions at 623 K and $P = 1$ atm. The catalytic activity of the dispersed carbide and nitride phases on the alumina carrier was more significant than that of the reference catalysts, alumina supported NiMo-S and CoMo-S. The metallic character of the NiMo and CoMo carbides was evidenced by their higher hydrogenation activity in thiophene HDS, while the nitrides favored both hydrogenation and hydrogenolysis type reactions.

Keywords: NiMo and CoMo carbides; NiMo and CoMo nitrides; Thiophene HDS; Dibenzothiophene HDS; HDS catalysts NiMo; CoMo carbide; Nitrides; Phosphorus promoters

1. Introduction

Stricter environmental regulations have driven the reduction of sulfur, nitrogen, and aromatics to a minimal level in fuels, a trend that will continue worldwide in the coming years, i.e., a target of about 15 ppm (0.0015 wt.%) in diesel by 2010 and sulfur reduction in gasoline reaching about 50 ppm (0.0050 wt.%) by 2006. Thus, in order to comply with these norms, the oil industry has been improving the performance of the hydrotreating (HDT) process, which is comprised of hydrodesulfurization (HDS), hydrodenitrogenation (HDN), hydrogenation (HYD), and hydrodemetallization (HDM). As the lower quality feedstock becomes more abundant or price attractive for refinery operations, additional challenges arise such as the transport and handling of heavier oil fractions, more severe operation conditions (T, P), higher corrosion of the refinery installations, catalyst deactivation and poisoning, etc. [1–4]. Therefore, one way to face these challenges is to develop catalysts that can better withstand the severe operation conditions prevailing in the HDT of heavier gasoils. Thus, the objective of the present study is to better understand the role of novel ceramic phases in the HDS of hydrocarbons, which could lead the way toward developing new catalysts with enhanced performance for HDT. Thus, a multifunctional approach was followed to consider the various individual components, i.e., the support, the active phases, and the promoters. In this respect, the refractory ceramic phases

* Corresponding author. Tel.: +52 8332158544; fax: +52 8332158544.
E-mail address: jaamelo@hotmail.com (J.A. Melo-Banda).

0920-5861/$ – see front matter © 2005 Elsevier B.V. All rights reserved.
doi:10.1016/j.cattod.2005.08.022

composed of bimetallic phases of NiMo- and CoMo-carbides and -nitrides dispersed on a carrier (gamma alumina) have been studied with increasing interest [5,6]. This is due not only to their high mechanical and thermal resistance, but also to the fact that these materials possess a significant catalytic activity for the hydrotreating of sulfur and nitrogen containing hydrocarbons [6–10]. For instance, Mo and W carbides and nitrides have demonstrated a performance for HDN and HYD type reactions that is comparable to some reference catalysts based on traditional $NiMoS/Al_2O_3$ [6,7]. However, some studies demonstrated that the catalytic properties of those refractory ceramic phases, i.e., (Ni,Co)-carbides and -nitrides, are strongly dependent on the presence of active MoS or mixed MoS/MoC surface layers. These layers may form under the reaction conditions [8] on the top surface of the Mo carbide phase, which may be responsible for the catalytic activity. Furthermore, the catalytic activity of the single-phase Ni, Co, and Mo carbides and nitrides seems closely related to their crystal structure and crystallite size [8,9]. Thus, in this work, γ-Al_2O_3 supported bimetallic NiMo and CoMo carbides and nitrides were synthesized, and the effects on their catalytic properties were explored using the HDS of thiophene as a model reaction. In particular, the effects of the atomic ratios and concentration of promoters (*P*) were sought. Finally, the effect of the phosphorus promoter was determined under high pressure conditions using the HDS of dibenzothiophene as a model reaction.

2. Experimental

The oxide precursors were prepared through incipient wetness impregnation of alumina ($S_g = 269\ m^2/g$) using the basic aqueous solutions with the appropriate salts at different atomic ratios, from 0.1 to 0.9. The support was obtained by calcining boehmite (CATAPAL) at 923 K with the precursor salts being: $Ni(NO_3)_2$, $Co(NO_3)_2$, and $(NH_4)_6Mo_7O_{24}{\cdot}4H_2O$ (Aldrich-Chemie). Phosphorous was incorporated using aqueous solutions of ammonium phosphate after drying the impregnated solids at 393 K (Aldrich-Chemie). All the samples were calcined at 773 K, and the metallic content in the samples is reported in Table 1. The synthesis of the NiMo and CoMo carbides and nitrides was carried out, as reported previously [8], by means of ammonolysis of the impregnated materials using a flow of NH_3 before the carburization stage in order to form the oxinitrides at 550 °C. At this temperature, a mixture of CH_4/H_2 was passed over the samples and the temperature was increased up to 973 K, then it was maintained for 1 h until obtaining the carbide phase. A similar procedure was used for the synthesis of the nitride phases using only the ammonia flow. Afterwards, samples were cooled down to room temperature and were ''passivated'' with flowing O_2/He (<1% O_2) to avoid the mass oxidation of the solids. The catalysts were characterized by X-ray diffraction (XRD) using a diffractometer, BRUKER-AXS, model D8 ADVANCE. Nitrogen adsorption was performed using an AUTOSORB-1 apparatus (QUANTA CHROME). The catalysts were evaluated for the HDS of thiophene at 623 K, $P = 1$ atm. Before the reaction, the materials were activated in situ under H_2 flow for 1 h at 673 K. Commercial HDS catalysts (NiMoS/ and $CoMoS/Al_2O_3$) were used as reference catalysts. The products were analyzed by gas chromatography, and the reaction rate was calculated according to the equation $Ra = FX/m$, where Ra is the HDS rate (mol g^{-1} s^{-1}), F the thiophene molar flow rate (mol s^{-1}), X the thiophene conversion, and m is the catalyst mass. This equation is reliable when the conversion is lower than 15%. Also, previous work allowed the authors to comply with the kinetic regime under the conditions used in this study. The more active catalysts (atomic ratios = 0.3 and 0.5, for nitrides and carbides, respectively) were tested in the HDS of dibenzothiophene in a batch reactor (450 ml) at 593 K, 800 psi, and 2000 rpm. In this case, the solvent used was hexadecane. The reaction products were mainly biphenyl and *cyclo*-hexylbenzene, which were analyzed using gas chromatography. The reaction rate constant was calculated from the experimental data by considering a pseudo first order reaction relative to DBT.

Table 1
Metallic atomic ratios and phosphorous content in the series of γ-Al_2O_3 supported nitride and carbide catalysts

Catalyst ($M^+/M^+ + Mo$)		Metal content (atom/nm^2)		Phosphorous (wt.%)
Nitrides	Carbides	M^+	Mo	
M^+-MoN-0.1	M^+-MoC-0.1	0.31	2.8	–
M^+-MoN-0.3	M^+-MoC-0.3	1.17	2.8	–
M^+-MoN-0.5	M^+-MoC-0.5	2.80	2.8	–
M^+-MoN-0.7	M^+-MoC-0.7	6.53	2.8	–
M^+-MoN-0.9	M^+-MoC-0.9	25.2	2.8	–
M^+-MoN-2.0	–	1.17	2.8	2.0
M^+-MoN-1.5	–	1.17	2.8	1.5
M^+-MoN-1.0	–	1.17	2.8	1.0
M^+-MoN-0.5	–	1.17	2.8	0.5
–	M^+-MoC-2.0	2.8	2.8	2.0
–	M^+-MoC-1.5	2.8	2.8	1.5
–	M^+-MoC-1.0	2.8	2.8	1.0
–	M^+-MoC-0.5	2.8	2.8	0.5
Sulfides				
$NiMoS/Al_2O_3$		1.17	2.8	1.69
$CoMoS/Al_2O_3$		1.19	2.8	1.70

M^+ = Ni or Co.

3. Results and discussion

3.1. Structural properties

Fig. 1 shows the X-ray diffraction patterns of the bimetallic CoMo carbide phases supported on γ-Al_2O_3, corresponding to the atomic ratios [Co/(Co + Mo)] = 0.1, 0.3, 0.5, 0.7, and 0.9. The characteristic peaks of the cobalt and molybdenum carbides are not apparent because the main γ-Al_2O_3 peaks overlap within the same 2θ interval. It is only at high metal contents that some peaks become clearly outlined. Some of the segregated carbide phases correspond to the molybdenum carbide phase (β-Mo_2C), which has a structure with hexagonal symmetry (J.C.P.D.S. card No. 43-1144) in which some characteristic peaks appear at 38.9°, 44°, and 74.3° (2θ). Also, a

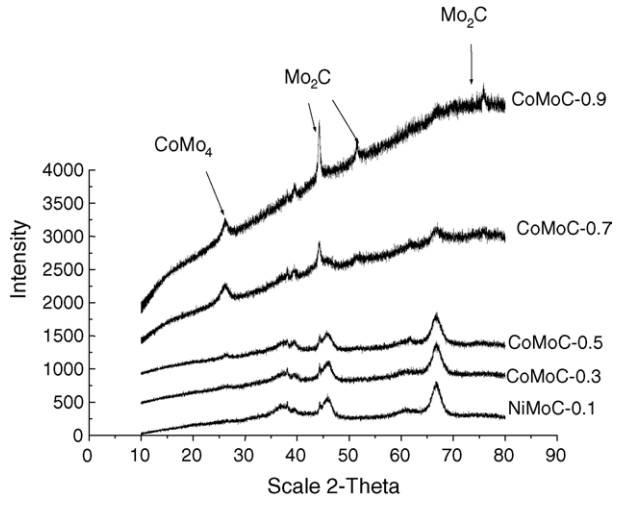

Fig. 1. Diffraction patterns of CoMo carbide phases supported on γ-Al_2O_3.

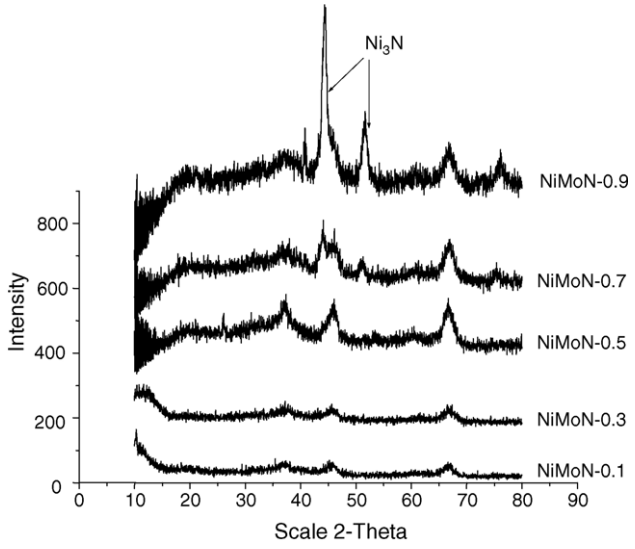

Fig. 3. Diffraction patterns of NiMo nitride catalysts supported on γ-Al_2O_3.

smaller peak corresponding to the Mo oxides was detected after a "passivation" treatment. Fig. 2 shows the XRD patterns corresponding to the NiMo carbide series with the same atomic ratios as the CoMo carbides. The XRD patterns of the samples having a lower metal concentration did not exhibit significant peaks; only the γ-Al_2O_3 phase (J.C.P.D.S. card No. 04-0875) was verified by the appearance of the typical XRD peaks at 38°, 46°, and 67° (2θ). Also, a prominent XRD peak corresponding to the Ni carbide was detected for the samples having an atomic ratio equal to 0.3.

Figs. 3 and 4 show the XRD patterns of the NiMo and CoMo nitride supported phases. All these diffraction patterns show the segregation of the single metal nitride phases, i.e., Ni_3N or CoN, probably as a consequence of their distinct heats of formation [10]. In spite of the support background in Fig. 3, the crystalline Ni_3N phase is apparent at 51° and 76° (2θ). Similarly, the XRD patterns of the CoMo nitride series show the presence of a CoN nitride phase at the higher ratios, i.e.,

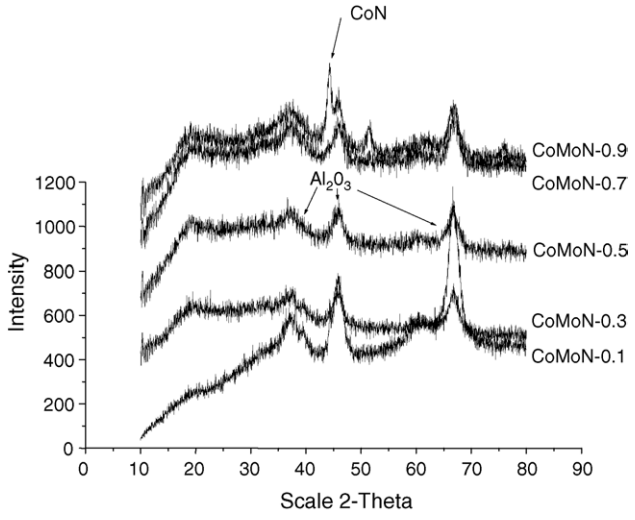

Fig. 4. Diffraction Patterns of CoMo Nitrides catalysts supported on γ-Al_2O_3.

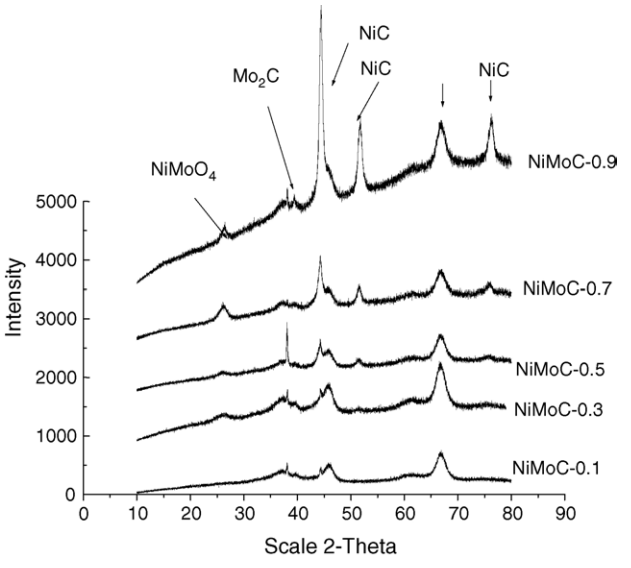

Fig. 2. Diffraction patterns of NiMo carbide catalysts supported on γ-Al_2O_3.

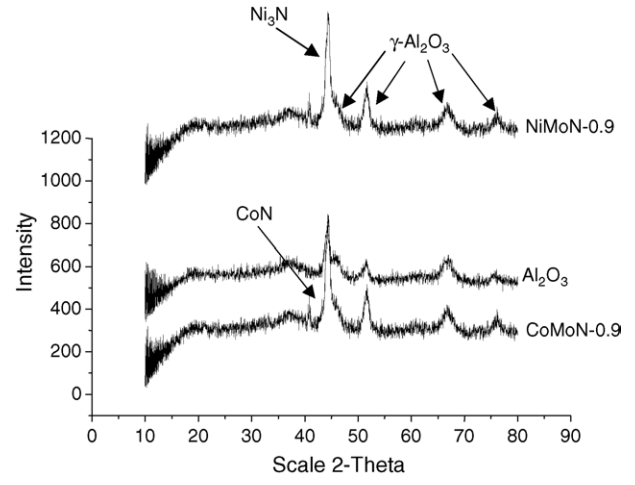

Fig. 5. XRD patterns of γ-Al_2O_3 supported CoMo and NiMo nitrides doped with 2 wt.%P.

Table 2
Surface areas of the (γ-Al_2O_3)-supported CoMo and NiMo nitrides and carbides

CoMo catalysts	Surface area (m^2/g)	Metal content (wt.%/g support)		NiMo catalysts	Surface area (m^2/g)	Metal content (wt.%/g support)	
		Co	Mo			Ni	Mo
CoMoN-0.1	227	0.63	9.14	NiMoN-0.1	192	0.54	7.85
CoMoN-0.3	226	2.34	8.95	NiMoN-0.3	187	1.97	7.55
CoMoN-0.5	224	5.39	8.6	NiMoN-0.5	193	4.71	7.56
CoMoN-0.7	220	11.5	7.91	NiMoN-0.7	210	11.04	7.62
CoMoN-0.9	212	32.7	5.81	NiMoN-0.9	208	30.71	5.47
CoMoC-0.1	254	0.70	10.11	NiMoC-0.1	247	0.68	9.86
CoMoC-0.3	248	2.54	9.71	NiMoC-0.3	239	2.45	9.40
CoMoC-0.5	244	5.8	9.25	NiMoC-0.5	199	4.84	7.76
CoMoC-0.7	109	6.32	4.35	NiMoC-0.7	153	8.47	5.85
CoMoC-0.9	105	20.15	3.57	NiMoC-0.9	157	26.88	4.79

Co/(Co + Mo) = 0.9. Also, a fluorescence effect was detected during the XRD experiments, which arises from the presence of cobalt in both the carbide and nitride phases.

Fig. 5 shows the XRD patterns of the supported NiMo- and CoMo-nitrides which contain about 2 wt.%P and a high metallic atomic ratio of approximately 0.9. The phosphorus compounds are not detected at all by XRD because of their low concentration. Also, the carbide phase is not shown in this figure because the peaks are masked by the support phase; thus, these results suggest that the carbides are highly dispersed on the alumina carrier. Moreover, the XRD patterns in Fig. 5 show the typical peaks of alumina together with the nickel and cobalt nitride phases.

3.2. Textural properties

The textural properties of the series are displayed in Table 2, where the complete range of atomic ratios is covered for both CoMo and NiMo catalysts. The surface area corresponding to the CoMo and NiMo nitride series was slightly lower than the γ-Al_2O_3 support, which is about 269 m^2/g. Nevertheless, the pronounced decrease in surface area sustained by the supported carbides can be attributed to the increase in the metallic concentration and to the formation of carbon fibers on the surface, which was verified by transmission electron microscopy observations [2,10–12].

3.3. Catalytic properties

3.3.1. Hydrodesulfurization of thiophene

The reaction rates for the NiMo and CoMo nitride series, which were determined according to previous reports, are illustrated in Figs. 6 and 7 [13,14]. The highest rate was obtained with the NiMoN-0.3 catalyst, which was comparable to the reference $NiMoS/Al_2O_3$ catalyst doped with phosphorous (1.69 wt.%P). The CoMo nitride series showed a behavior similar to the NiMo nitrides. In Figs. 6 and 7, one observes that the catalytic activity of the nitrides varies inversely with respect to the atomic metal ratios; thus, the HDS conversion increases for those nitride materials having the lesser atomic ratios. This behavior could be attributed to the formation of crystal clusters, as shown by the XRD results. Also, at the beginning of the catalytic reaction, the materials having an atomic ratio around 0.3 had the highest activity. In particular, in the CoMo and NiMo nitride series the NiMoN-0.3 catalysts were more active than the CoMoN-0.3. On the other hand, Fig. 8 shows a

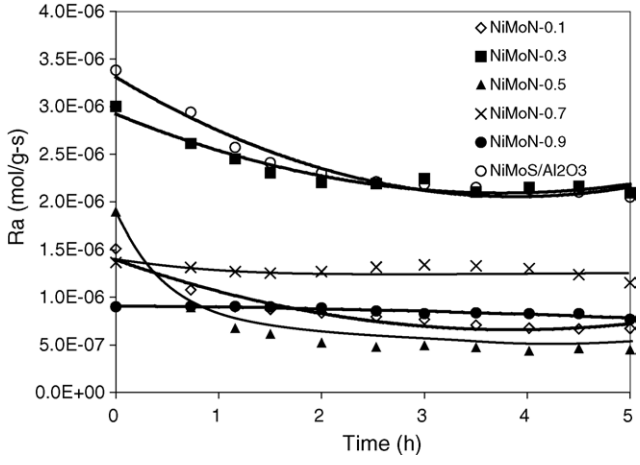

Fig. 6. Variation of reaction rates with time-on-stream for the supported NiMo nitride catalysts in the HDS of thiophene at 623 K and 1 atm.

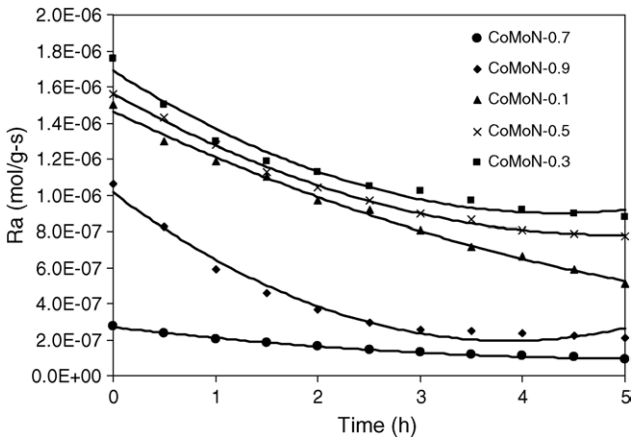

Fig. 7. Variation of reaction rates with time-on-stream for the supported CoMo nitride catalysts in the HDS of thiophene at 623 K and 1 atm.

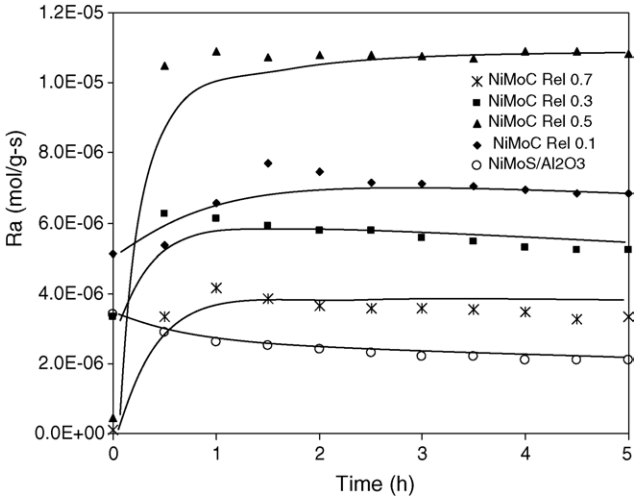

Fig. 8. Variation of reaction rates with time-on-stream for the NiMo supported carbide catalysts in the HDS of thiophene at 623 K and 1 atm.

comparison of the various reaction rates as a function of the time-on-stream, corresponding to the NiMo carbide series and the $NiMoS/Al_2O_3$ reference catalysts. For the $NiMoC/Al_2O_3$ carbide series, the most active catalyst was NiMoC-0.7, but in general, the catalytic activity of the carbide catalysts was superior to that of the alumina sulfided catalysts. There is a possibility that binary phases could be formed between the metal sulfides and carbides, which would further contribute to the enhanced activity. However, the XRD analysis of the catalysts after the reaction test did not show the sulfided phases to be present [15]. Fig. 9 shows the variation of the activity with time-on-stream corresponding to the CoMo carbide type catalysts, where one observes that their activity level is very similar to the supported nitride phases at the same level of metal concentration. However, there seems to be a lesser activity than that of the bimetallic sulfides (Fig. 9). The catalysts with atomic ratios equal to 0.1 and 0.7 did not show any activity under the conditions used. Overall, the most active catalysts for thiophene HDS (Fig. 10) were the supported bimetallic NiMo and CoMo nitrides; two sets appear, separated from each other by the highest and the regular activity level. If one compares the

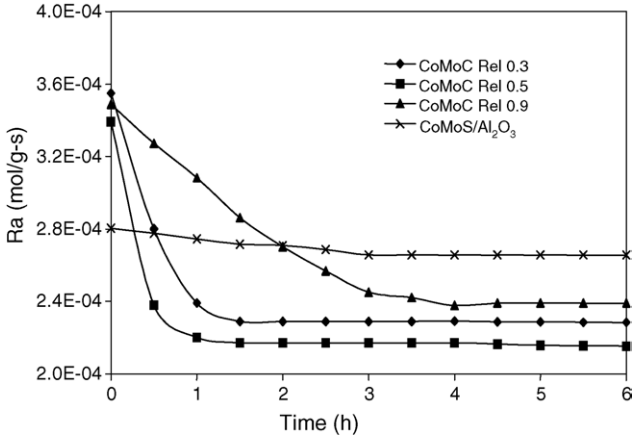

Fig. 9. Variation of reaction rates with time-on-stream for the CoMo supported carbide catalysts in the HDS of thiophene at 623 K and 1 atm.

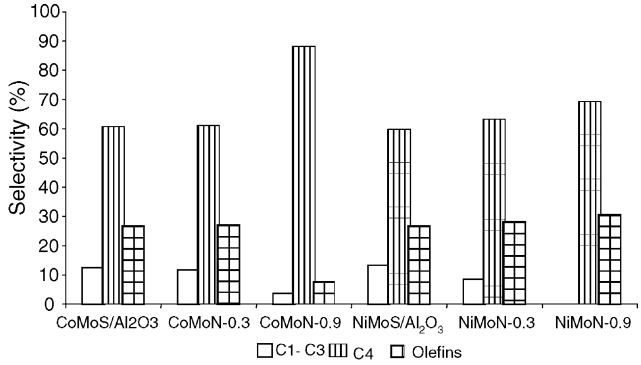

Fig. 10. Selectivity of CoMo and NiMo supported nitride catalysts in the HDS of thiophene.

selectivity values at the same conversion level for all the samples, it is apparent that the hydrogenation activity of the nitride series prevails over the one corresponding to the $NiMoS/Al_2O_3$ catalysts. The supported NiMoN and CoMoN catalysts series showed a significant hydrogenation and hydrogenolysis activity, with a higher selectivity toward the formation of *n*-butane and olefins, i.e., *cis*-2 butane, *trans*-2 butene, and 1-butene [14]. However, the supported carbides were more prone to hydrogenation, which is attributed to their proper structural arrangements and metallic character [10,16,17]. The supported carbide series showed a selectivity mainly toward *n*-butane (i.e., Figs. 11 and 12), while the proportion of the other products, like the ones derived from cracking or the branched double and tri-bonded hydrocarbons, are minor. Also, the NiMoN-0.3 and NiMoN-0.5 catalysts, similarly to the NiMo sulfides, were the only ones in the series that favored both hydrogenation and hydrogenolysis, although some specific compositions in both series, i.e., the NiMo-0.5 bimetallic carbides and nitrides, have a significant activity level for HDS type reactions.

3.3.2. Hydrodesulfurization of dibenzothiophene

In order to verify whether or not a correlation exists between the carbides and nitrides used in the HDS of dibenzothiophene, four series of materials were prepared and tested for their catalytic activity, corresponding to atomic ratios of 0.3 and 0.5 for nitrides and carbides, and a phosphorous composition

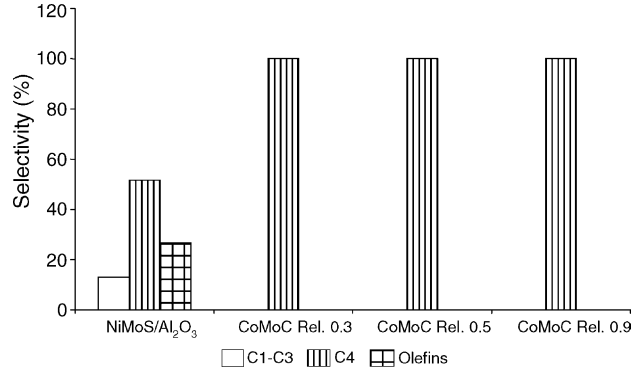

Fig. 11. Selectivity of supported CoMo carbide catalysts in the HDS of thiophene.

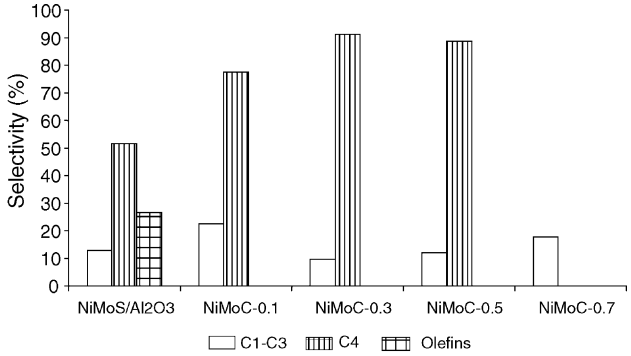

Fig. 12. Selectivity of supported NiMo carbide catalysts in the HDS of thiophene.

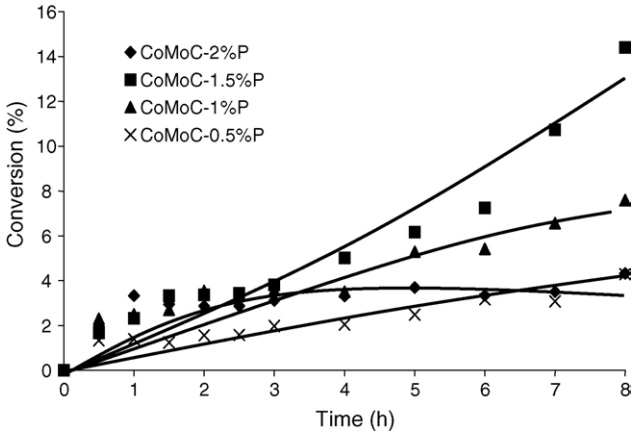

Fig. 14. Variation of conversion with time-on-stream in the HDS of DBT for the supported CoMo carbide catalysts with different phosphorus content at 593 K and 800 psi.

varying between 0.5 and 2.0 wt.%. The results obtained with the nickel-molybdenum carbide series (i.e., NiMoC-2, 1.5, 1, and 0.5 wt.%P) are illustrated in Fig. 13. There, one observes that the NiMoC-1.5 wt.%P catalyst showed the highest conversion (about 22%) with respect to this series, the main product being biphenyl (BP). Also, the CoMo carbide series showed that the catalyst having 1.5 wt.%P, CoMo-1.5, presented the highest conversion (about 15%) after 8 h on stream, although it did not follow a pseudo first order kinetics, as observed in Fig. 14. According to the current literature, the catalysts having a phosphorous content similar to commercial catalysts, i.e., 1.5–1.69 wt.%P, show a similar behavior in the HDS of DBT; this suggests that a synergism occurs between the active phases, regardless of the anionic component in the bimetallic compounds, i.e., carbides, nitrides, or the sulfided phases. On the other hand, Fig. 15 shows the variation of the conversion (HDS) of DBT that corresponds to the supported NiMo nitride series (NiMoN-2, 1.5, 1, and 0.5 wt.%P); there, one observes that the highest conversion is shown by NiMoN-1.5 wt.%P, at about 50% conversion, after 8 h on stream. A similar behavior was observed with other catalysts in this series that had the same phosphorous content. The lower activity level was shown by the catalysts having a phosphorous loading of 2 wt.%, which can be attributed to the excess concentration of phosphorous on the surface of these solids. This excess could favor the formation of crystalline phosphates that may cause a decrease in the surface area due to the pores blockage [18,19]. Furthermore, the presence of the phosphate ions could change the nature of both nickel and molybdenum phases at the surface level, but the overall amount of these phosphate compounds is too small to be identified by XRD.

In contrast with the previous cases, the first catalyst in the nitride series, CoMoN-0.5 wt.%P, showed the highest activity level, 17% after 8 h on stream; the CoMoN-1.5 wt.%P presented a conversion smaller than that of CoMoN-2 wt.%P (i.e., 12% conversion). On the other hand, Table 3 illustrates the reaction rates that were calculated as the DBT disappears, considering a pseudo first order equation. In the series of NiMo carbides (i.e., NiMoC-2, 1.5, 1, and 0.5 wt.%P), the catalytic activity had a similar magnitude, although the NiMoC-1.5 catalyst, being 2.8 times more active than the NiMo-1.0 catalyst, showed the highest activity. Similarly, the CoMo carbides presented the same behavior when they had the same phosphorous concentration (1.5 wt.%P). This catalyst was 5.25 times greater than the least active catalyst in the series (i.e., CoMoC-2.0). In turn, in the nitride series, the P-promoted

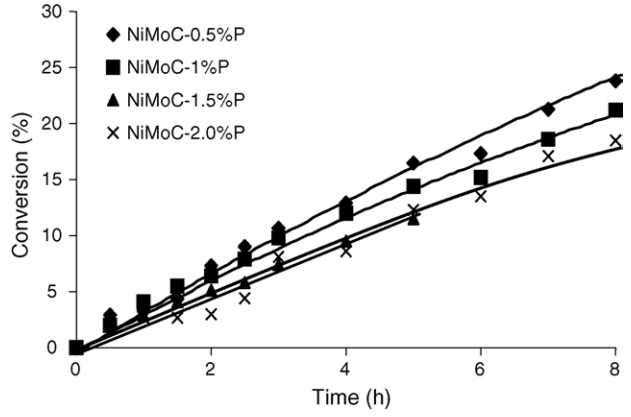

Fig. 13. Variation of conversion with time-on-stream in the HDS of DBT for the supported NiMo carbide catalysts with different phosphorus content at 593 K and 800 psi.

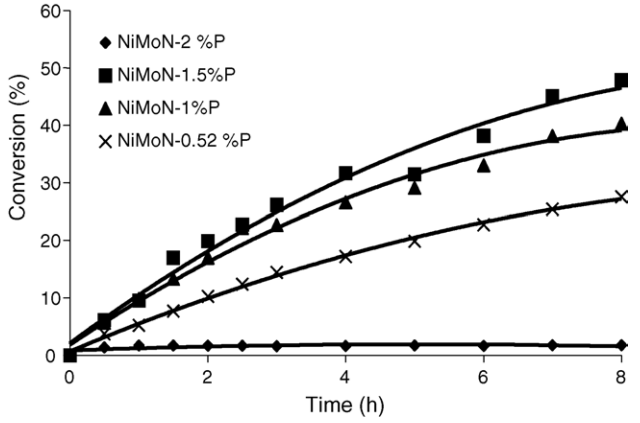

Fig. 15. Variation of conversion with time-on-stream in the HDS of DBT for the supported NiMo nitride catalysts with different phosphorus content at 593 K and 800 psi.

Table 3
Effect of phosphorous content on pseudo first order rate constants for HDS of DBT on NiMo and CoMo carbide and nitride species, at 593 K and 800 psi

Catalysts	$k \times 10^{-4}$ (m^3/kg catalyst min)	Catalysts	$k \times 10^{-4}$ (m^3/kg catalyst min)
NiMoC-2.0%P	2.14	CoMoC-2.0%P	0.24
NiMoC-1.5%P	4.06	CoMoC-1.5%P	1.26
NiMoC-1.0%P	1.44	CoMoC-1.0%P	0.61
NiMoC-0.5%P	2.76	CoMoC-0.5%P	0.35
NiMoN-2.0%P	0.07	CoMoN-2.0%P	1.09
NiMoN-1.5%P	6.66	CoMoN-1.5%P	0.97
NiMoN-1.0%P	5.20	CoMoN-1.0%P	0.81
NiMoN-0.5%P	5.61	CoMoN-0.5%P	1.89

catalysts (i.e., NiMoN-2, 1.5, 1, and 0.5 wt.%P) exhibited a profile similar to that of the carbide series; however, the NiMoN catalysts were more active for the HDS of DBT. In fact, the catalyst NiMoN-1.5 was twice as active as its closest follower in the same series. In general, the CoMo based nitride catalysts showed a lesser activity than all the other series (Fig. 16).

The composition of the reaction products changed with the composition of the bimetallic nitrides and carbides. For example, the biphenyl and *cyclo*-hexylbenzene (CHB) were two reaction products, the former being more common, but the latter appeared only in the presence of the NiMoC-1.0 catalyst. A similar behavior was shown by the carbide series (Fig. 17). The BP can be formed directly by the hydrogenolysis of C–S bonds, but the CHB may be derived from three pathways: the hydrogenation of BP, the desulfurization of tetra-hydrodibenzothiophene (THDBT), or the desulfurization of hexa-hydrodibenzothiophene (HHDBT). The latter compound does not appear among the products [20], which could indicate that the desulfurization rate is faster than the hydrogenation rate. Fig. 18 illustrates the behavior of the CoMoC-1.0 catalyst, which represents the behavior of the supported carbides, where the selectivity was mostly oriented towards BP, but where a small amount of CHB forms as well. The NiMoN-1.5 and CoMoN-1.0 catalysts representing the NiMo and CoMo nitrides series (Figs. 19 and 20, respectively) shows that bi-

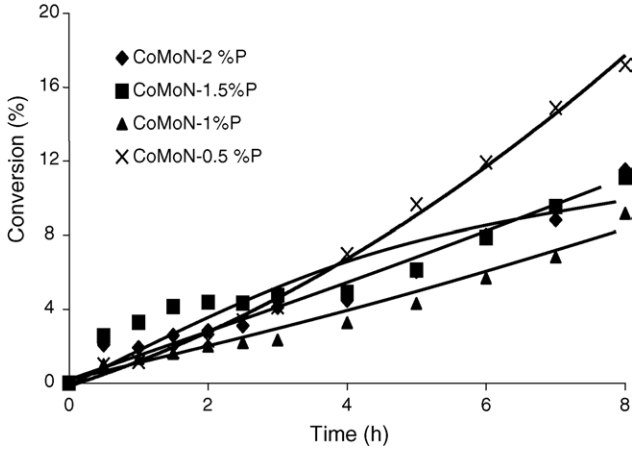

Fig. 16. Variation of conversion with time-on-stream in the HDS of DBT for the supported CoMo nitride catalysts with different phosphorus content at 593 K and 800 psi.

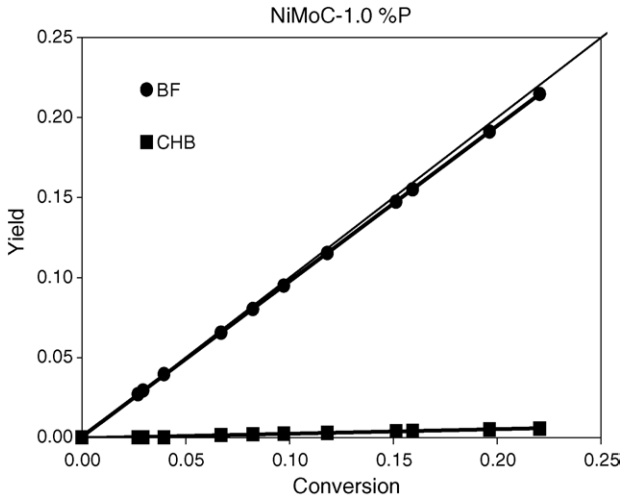

Fig. 17. Products yield as a function of conversion for the supported NiMoC-1.0%P in the HDS of DBT at 593 K.

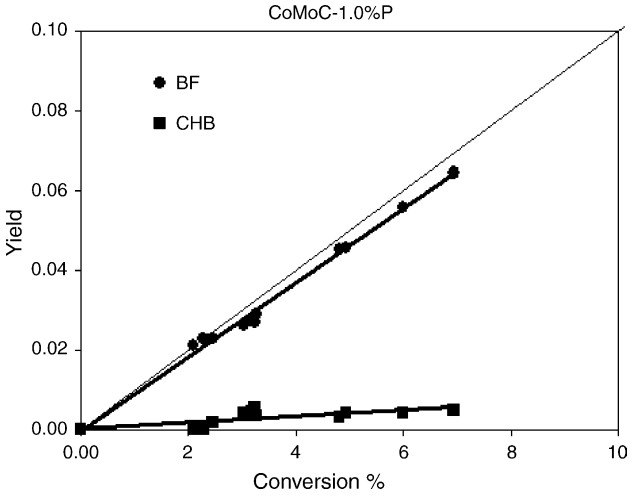

Fig. 18. Products yield as a function of conversion for the supported CoMoC-1.0%P in the HDS of DBT at 593 K.

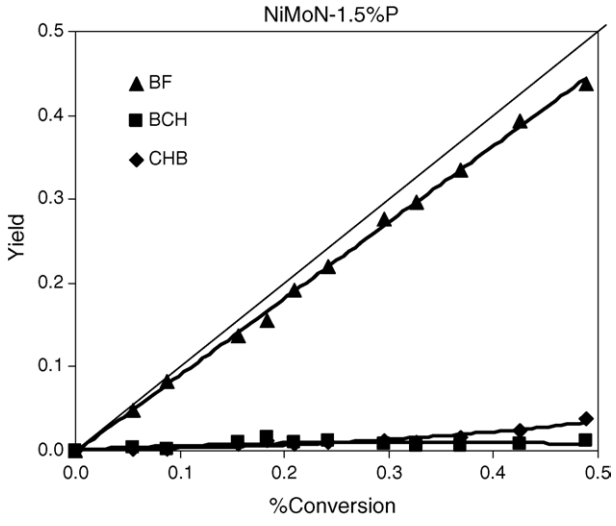

Fig. 19. Products yield as a function of conversion for the supported NiMoN-1.5%P in the HDS of DBT at 593 K.

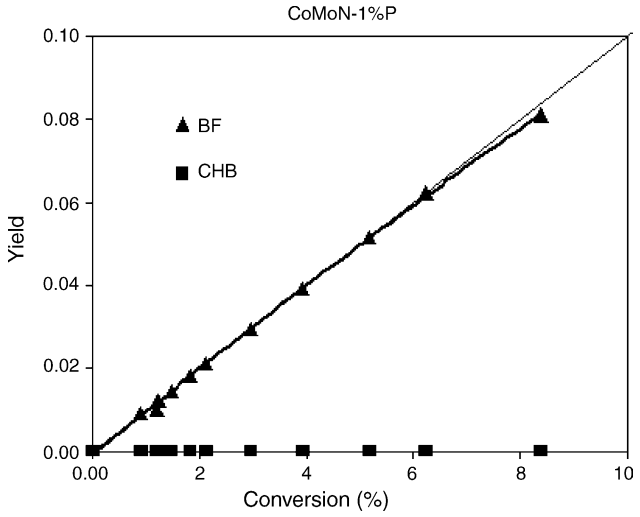

Fig. 20. Products yield as a function of conversion for the supported CoMoN-1%P in the HDS of DBT at 593 K.

cyclohexyl (BCH) was formed in addition to BP and CHB, which indicates that there is no deep hydrogenation of dibenzothiophene through the formation of per-hydrodibenzothiophene to produce bi-cyclohexyl as described elsewhere [21]. In general, these results suggest that the nitride type catalysts were more active and highly selective toward sulfur removal. The reaction seems to take place by the direct C–S hydrogenolysis of dibenzothiophene to biphenyl before the DBT hydrogenation, followed by the sulfur removal.

4. Conclusions

The synthesis of supported NiMo and CoMo carbides was carried out by the ammonolysis and subsequent carburization of the metal phases from methane decomposition onto dispersed metal salts impregnated by the γ-Al_2O_3 support. The NiMo and CoMo nitride series were prepared by direct ammonolysis. The XRD characterization of the Ni-Mo and Co-Mo carbides and nitrides showed a segregation of phases, i.e., β-Mo_2C and NiC in the carbide systems, and Ni_3N and CoN in the nitride systems. This segregation is a consequence of the distinct heats of formation of these carbide phases [10], and this causes the catalysts to consist of both mixed Ni-Mo and Co-Mo phases together with single Ni, Mo, and Co carbides and nitrides, respectively. However, the formation of small crystals of metal carbides and nitrides supported on the alumina carrier might lead to the loss of surface area, most probably due to pore blockage. In the HDS of thiophene, the catalytic properties of the dispersed refractory phases were generally outstanding with respect to the reference catalysts based on $NiMoS/Al_2O_3$. In particular, these effects were more evident in the series of NiMo carbide and nitride catalysts whose atomic ratios were equal to 0.5 and 0.3, respectively. Both series showed a significant activity level for hydrogenation and hydrogenolysis reactions; consequently, these were more selective toward the formation of *n*-butane and olefins from the HDS of thiophene. In general, the catalytic behavior of the unsupported single-phase carbides and nitrides is attributed mainly to their particular electronic structure in which the carbon and nitrogen atoms occupying the interstices should contribute to the unit cell parameter's expansion (i.e., hexagonal close-packed or body centered cubic for Mo carbides and Mo nitrides, respectively) and add electrons to the d-orbitals, thus enhancing the metallic character of the transition metal carbides/nitrides. However, the supported bimetallic NiMo and CoMo carbides and nitrides are more complex systems by far with respect to the unsupported single-phase counterparts, and, at present, they have not been fully characterized. This complexity increases if one considers the possible inclusion of oxygen atoms inside the lattice, thus forming oxycarbides or oxynitrides. In addition, as the segregation of single phases occurs, the effects of a specific type of active sites are masked. Therefore, at this point the present work is limited to the exploration of the catalytic behavior with respect to thiophene and dibenzothiophene HDS only; however, the general features of the catalysts such as the texture and crystallographic structure are provided in order to search for a correlation between these data and further studies. Also, it was observed that the catalysts containing 1.5 wt.%P were more active, with the exception of the case of CoMo nitrides, thus indicating that phosphorous is acting like a promoter as it does it in the metal sulfides (i.e., NiMoS and CoMoS). One of the promoting functions of phosphorus consists in favoring metal dispersion (i.e., Ni, Co, and Mo), thus increasing the number of oxide type nuclei that play the role of precursors for the formation of small carbide and nitride crystals. In turn, the dispersion of these metal precursors depends on the synthesis conditions. Although higher amounts of P are generally favorable for the catalytic activity of conventional catalysts, a content of phosphorous greater than 2 wt.% provoked deleterious effects on the catalytic performance of the refractory phases, possibly due to the formation of alternate phosphates on the top surface of the solids. Also, it was observed that the selectivity toward the formation of biphenyl occurred through the direct desulfurization of DBT, but a small amount of other products such as *cyclo*-hexylbenzene and bi-cyclohexyl also formed. This behavior coincides with the one observed for the $NiMoS/Al_2O_3$ and $CoMoS/Al_2O_3$ systems, which has been explained as the result of the formation of some promoted species like MoS, when Ni and Co are present in a form such as CoMo-S or NiMo-S. The selectivity in these cases seems substantially different to the one observed in the non-promoted systems.

References

[1] R. Cuellar, R. Zárate, O. Bermúdez, X Simp. Iberoam. Catal. 3 (1988) 1227–1232.
[2] J.S. Lee, T. Oyama, M. Boudart, J. Catal. 106 (1987) 125–133.
[3] J.S. Lee, L. Volpe, F.H. Ribeiro, M. Boudart, J. Catal. 112 (1988) 44–53.
[4] M. Nagai, T. Miyao, Catal. Lett. 3 (1999) 105–109.
[5] M. Vrinat, M. Breysse, C. Geantet, J. Ramirez, F. Massoth, Catal. Lett. 26 (1994) 25–35.
[6] P. Aerter, W. Quigley, D. Ziegler, J. Logan, M. Burell, J. Catal. 164 (1996) 119–121.
[7] S. Lobos, A. Martínez, F. Arenas, L. J. Brito, Proceedings in Electronic Version of XVII Simp. Iber. Catal., Porto, Portugal, 2000.

[8] J.A. Melo, J.M. Dominguez, G. Sandoval, Catal. Today 65 (2001) 279–284.
[9] J.A. Melo, Ph.D. Thesis (In Spanish), ITCM, México, 2000.
[10] E. Furimsky, Appl. Catal. A 240 (2003) 1–28.
[11] A. Griboval, P. Blanchard, E. Payen, M. Fournier, J.L. Dubois, J.R. Bernard, Appl. Catal. A 217 (2001) 173–183.
[12] S. Wanner, L. Hilaire, P. Wehrer, J.P. Hindermann, G. Maire, Appl. Catal. A 203 (2000) 55–70.
[13] M. Vrinat, Appl. Catal. 6 (1983) 137–158.
[14] M.J. Girgis, B.C. Gates, Ind. Eng. Chem. Res. 30 (1991) 2021–2058.
[15] T.A. Reyes, J.A. Melo, R. Garcia, J.M. Domínguez, J. Phys.: Condens. Matter 16 (2004) S2329–S2334.
[16] G. Berhault, A. Mehta, A.C. Pavel, J. Yang, L. Rendon, M.J. Yacaman, L. Cota Araiza, A. Duarte Moller, R.R. Chianelli, J. Catal. 9 (2001) 198.
[17] R. Cowan, M. Hoglin, H. Reinink, J. Jsebaert, D. Chadwick, Catal. Today 45 (1998) 381–384.
[18] P. Atasanova, T. Halachev, J. Uchetil, A. Lopez-Agudo, Appl. Catal. 161 (1997) 105.
[19] J. Ramirez, V.M. Castaño, C. Leclecq, A. Lopez-Agudo, Appl. Catal. 62 (1992) 251.
[20] J. A. de los Reyes, J. A. Colin, E. Altamirano, B. Jouget, M. Vrinat, C. Geantet, Proceedings of XVIII Simp. Iber. Catal., Isla Margaritas, Venezuela, 2000, pp. 821–826.
[21] M. Nagai, T. Satoh, A. Aiba, J. Catal. 97 (1986) 52.